IS-T 1734

Design and Construction of a RHEED Diffractometer with Energy Resolution Capability

by

Formas, Rodrigo

MS Thesis submitted to Iowa State University

Ames Laboratory, U.S. DOE
Iowa State University
Ames, Iowa 50011

Date Transmitted: February 10, 1995

PREPARED FOR THE U.S. DEPARTMENT OF ENERGY
UNDER CONTRACT NO. W-7405-Eng-82.

DISCLAIMER

TABLE OF CONTENTS

INTRODUCTION

The study of surfaces and interfaces in a solid is of great importance for the understanding of its basic properties. Even though at least one in 10^8 atoms resides near the surface, properties such as the work function, originating from the bulk part of a solid, are in part determined by surface conditions. This is because the distortions in the electronic charge distribution near the surface affect the energy levels far inside the solid via the long range Coulomb interaction. Since most solid state electronic devices involve removal of electrons from a solid, or passage from one solid to another, it is of primary importance to understand surface phenomena (1).

In a solid, the geometrical arrangement of surface atoms largely determines the near-surface charge and spin density. However, the surface structure in a solid can be different than the bulk structure. For this reason, many experimental approaches to surface structural analysis have been developed. For the bulk part of a solid, structural analysis is normally resolved by x-ray diffraction. However, the large penetration depth and mean free path of x-rays make them unsuitable for routine use in surface crystallography, except under special circumstances (grazing angles of incidence with synchrotron x-ray sources). A better approach to the problem consists of using electrons with small de Broglie wavelengths (typically 1Å) to perform electron diffraction. Two diffraction techniques, LEED and RHEED, and STM Imaging will briefly be discussed.

In LEED (Low Energy Electron Diffraction) electrons in the energy range $50<E<500$ eV are coherently reflected from the topmost atomic layer of a crystalline solid. The technique is surface sensitive because elastically scattered electrons of low energies penetrate only a very short distance into the solid, and the diffraction pattern is determined almost entirely by the surface atoms (5). Figure 1 illustrates a typical arrangement for LEED. Electrons strike the surface at an angle close to the normal and some backscatter towards the hemispherical grid-screen arrangement. Biasing the grids

allows the passage of only elastically scattered electrons towards the screen. The LEED pattern thus formed is an image of the surface reciprocal net. Unfortunately, this technique does not allow for in-situ measurements, such as epitaxial growth, during growth processes.

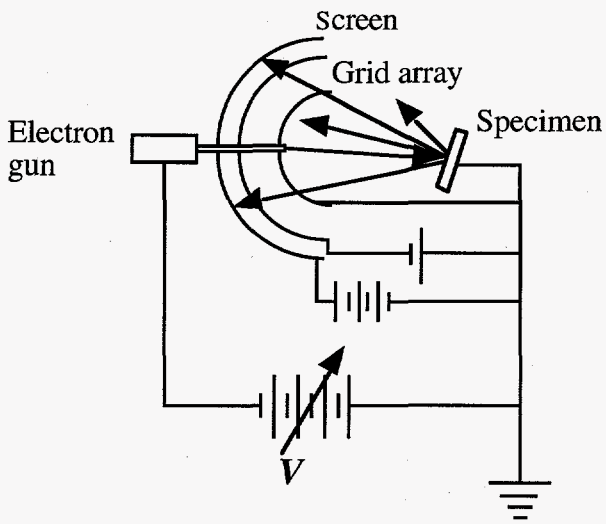

Figure 1. A typical LEED system

Another technique, that can be used for in-situ measurements during growth experiments, is RHEED (Reflection High Energy Electron Diffraction). The energy of the electrons is in the range 5<E<100 KeV. In RHEED, the incident electron beam strikes the surface of a specimen at grazing incidence ($\theta_i < 5^\circ$). With atomically flat surfaces, the penetration of the electron beam in a direction perpendicular to the surface is very small, and only a few monatomic layers contribute to produce coherently diffracted electrons. RHEED techniques are particularly useful for epitaxial growth because, apart from the improved accessibility to the surface in the normal direction relative to LEED, the use of small incidence angles makes the technique sensitive to the quality of the microscopic surface; grazing incidence electrons will penetrate into

asperities on the surface if it is not microscopically flat. This implies more careful sample preparation for RHEED studies, but the technique can identify changes in surface morphology.

Scanning Tunneling Microscopy has made it possible to virtually look at the real space geometry of a surface with atomic resolution. A sharp metallic tip is held at about 6 Å above the sample surface so that the wave functions of electrons in the sample and tip overlap, causing a small electron tunneling current to flow when a small voltage (0-2 V) is applied. In the constant current mode, the tunneling current is kept constant by feeding back a correction voltage that changes the position of the tip above the surface. Thus, a measure of the corrugation or topography of the surface is obtained. Unfortunately, the STM cannot yield in-situ measurements during growth processes.

In this work we describe the set up of a UHV system to study the growth of ultra-thin metallic films on a silicon substrate under RHEED conditions. However, a new feature has been added to the normal RHEED apparatus. Because the phosphor screen acts as a high pass filter for the scattered electrons, energy filtering is normally excluded from RHEED techniques. In our experimental apparatus, a biased Faraday collector has been added to measure only the elastically scattered part of the diffracted beams. The electrical currents involved range from about 15 nA to 0.1 nA for the elastically scattered part of a diffracted beam(6). The (111) surface of Si has been chosen to perform RHEED, with the incident beam along the (100) direction (see Figure 2).

Si STRUCTURE

Bulk Structure

Silicon has a diamond structure with lattice constant a=5.43 Å . This lattice consists of two interpenetrating FCC lattices displaced along the body diagonal of the cubic cell by one quarter the length of the diagonal. Therefore, the Si crystalline structure can be regarded as an FCC lattice with the two point basis, 0 and $(a/4)(\hat{x}+\hat{y}+\hat{z})$.

Si(111) Surface

The Si(111) surface is shown in Figure 2. It consists of a hexagonal lattice with primitive vectors $\vec{a}_1$ and $\vec{a}_2$. By choosing a coordinate system with axes along the principal directions of the surface, the primitive vectors can be expressed as

$$\vec{a}_1 = \frac{\sqrt{2}}{2}a\hat{x}; \quad \vec{a}_2 = \frac{\sqrt{2}}{4}a\left(\hat{x}+\sqrt{3}\hat{y}\right).$$

This structure is commonly referred as to the Si(111) 1×1 surface.

Si(111) 7×7 Structure

When a Si(111) surface is heated above 1200°C, a reversible transformation takes place, giving origin to a periodic structure referred as to the Si(111) 7×7 structure[3]. As the nomenclature suggests, the periodicity of this structure can be described by lattice vectors in the same direction but seven times longer than those used to describe

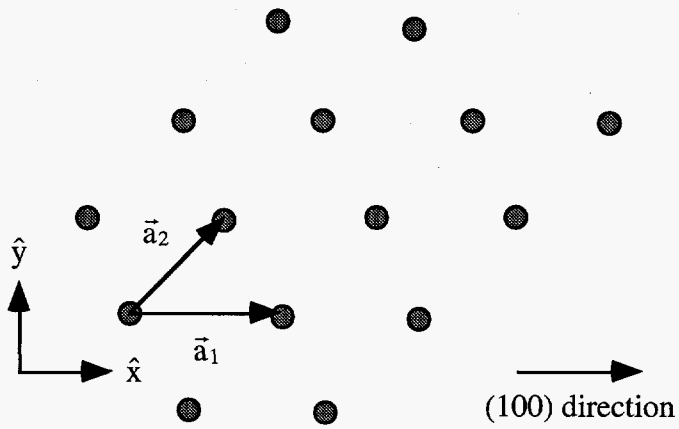

Figure 2. Si(111) surface

the Si(111) 1×1 structure. The most important structural features of the 7×7 structure that can be seen in Figure 3 are[9]:

1) Twelve top layer adatoms

2) A stacking fault in one of the two triangular subunits of the second layer

3) Nine dimers that border the triangular subunits in the third layer

4) A deep vacancy at each apex of the unit cell

The surface unit cell contains 12 atoms in the first layer, 42 atoms in the second layer and 60 atoms in the third layer. The Si(111) 7×7 structure is believed to be a clean surface structure; therefore, it can be used to check for cleanliness and smoothness of the specimen surface.

Si(111)-$\sqrt{3}\times\sqrt{3}$ R 30°-Ag Structure

There are several surface structures that can be induced by evaporation of a metal unto a Si(111) surface. In particular, the evaporation of Ag on Si(111) has been

o Top layer
● Second layer
• Third layer

Figure 3. The Si(111) 7×7 unit cell

extensively studied using several techniques. The surface structure formed after deposition of Ag/Si(111) depends upon the annealing temperature and the amount of Ag deposited. The $\sqrt{3} \times \sqrt{3}$ structure can be obtained with annealing temperatures between 290°C and 610°C and coverages above 0.1 ML[3].

RECIPROCAL LATTICE AND RHEED IN Si(111)

It has been pointed out already that diffraction techniques are useful to study the structure of crystalline solids. Information about the translational symmetry is usually acquired by mapping the reciprocal lattice of the solid. For instance, it was noted that the LEED pattern of a surface is a replica of its reciprocal net. Thus the concept of reciprocal lattice plays a fundamental role in diffraction studies. This is not true of diffraction techniques only, but of many other analytic studies of periodic structures.

Reciprocal Lattice

A three-dimensional Bravais lattice is a set of points with position vectors $\vec{R}$ given by

$$\vec{R} = n_1\vec{a}_1 + n_2\vec{a}_2 + n_3\vec{a}_3$$

where $\vec{a}_1, \vec{a}_2$, and $\vec{a}_3$ are any vectors, not all coplanar, and n_1, n_2, and n_3 are integers(1). The primitive vectors $\vec{a}_i$ are said to generate the Bravais lattice. In other words, a Bravais lattice is a discrete set of vectors not all coplanar, closed under vector addition and subtraction. With a given Bravais lattice, we can associate a reciprocal lattice. Consider a plane wave, $e^{i\vec{k}\cdot\vec{r}}$. The set of all wave vectors $\vec{K}$ that yield plane waves with the periodicity of the Bravais lattice is known as its reciprocal lattice. Thus, the set of points $\vec{R}$ of a Bravais lattice and $\vec{K}$ of its reciprocal lattice satisfy the relation

$$e^{i\vec{K}\cdot(\vec{r}+\vec{R})} = e^{i\vec{K}\cdot\vec{r}}$$

for all $\vec{r}$. It can be shown[1] that if $\vec{a}_1, \vec{a}_2$, and $\vec{a}_3$ constitute a set of primitive vectors for the direct lattice, the reciprocal lattice can be generated by the three primitive vectors

$$\vec{b}_1 = 2\pi \frac{\vec{a}_2 \times \vec{a}_3}{\vec{a}_1 \cdot (\vec{a}_2 \times \vec{a}_3)},$$

$$\vec{b}_2 = 2\pi \frac{\vec{a}_3 \times \vec{a}_1}{\vec{a}_1 \cdot (\vec{a}_2 \times \vec{a}_3)},$$

$$\vec{b}_3 = 2\pi \frac{\vec{a}_1 \times \vec{a}_2}{\vec{a}_1 \cdot (\vec{a}_2 \times \vec{a}_3)}.$$

The results described so far can be easily applied to surfaces of crystalline solids. Since these systems are two-dimensionally periodic, only two primitive vectors are required to describe the direct lattice. The reciprocal lattice is also two-dimensionally periodic, but it is replaced by infinite reciprocal lattice rods perpendicular to the surface and passing through the reciprocal net points. Qualitatively, this can be realized by noticing that distances in reciprocal space are inversely proportional to distances in real space. Thus the continuous increase in the distance between atomic planes along an axis in real space leads to closer planes along this axis in the reciprocal lattice. In the limit, when all planes have been removed to infinity one is left only with a single plane, and the reciprocal lattice becomes a set of infinitely long rods normal to the plane of atoms. A representation of such a reciprocal lattice is shown in Figure 4.

RHEED from Si(111)

It has been previously noted that diffraction techniques give information about the translational symmetry of a system in the form of the reciprocal lattice. When a diffraction process involving a surface occurs, the diffracted beams that result can be

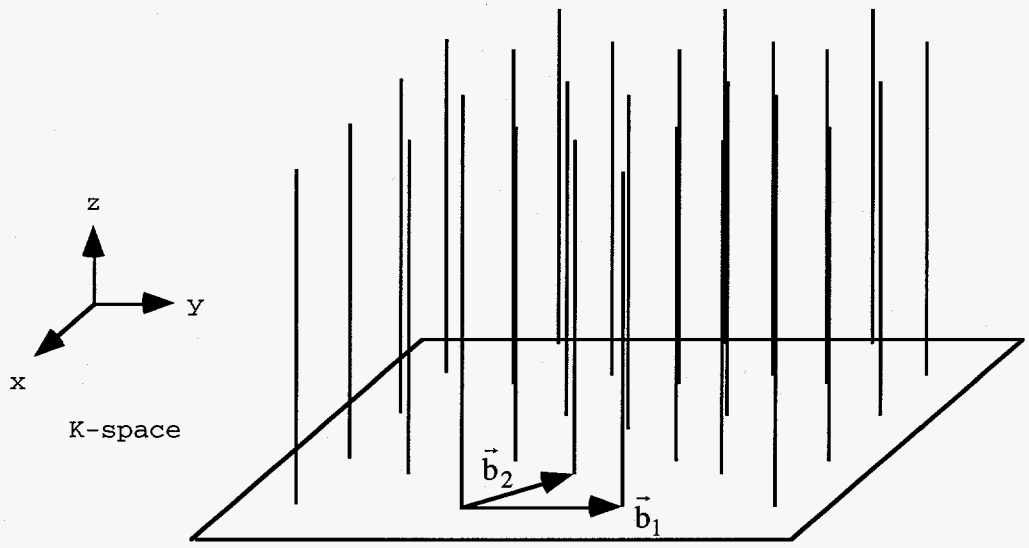

Figure 4. The reciprocal lattice of a two-dimensional surface

easily explained in terms of conservation of energy and conservation of momentum parallel to the surface, but only for the addition of any reciprocal lattice vector(7). Thus, if the incident wave vector is $\vec{k}$ and the emerging wave vectors are $\vec{k}'$, conservation of energy gives

$$k^2 = k'^2$$

while conservation of momentum parallel to the surface gives

$$\vec{k}'_{\parallel} = \vec{k}_{\parallel} + \vec{g}_{hk}$$

where

$$\vec{g}_{hk} = h\vec{b}_1 + k\vec{b}_2$$

is a reciprocal lattice vector with h and k integers.

A particularly useful graphical representation of these equations is the Ewald sphere construction. This is shown in Figure 5. The construction, superimposed on the reciprocal lattice, involves drawing a vector $\vec{k}$ terminating at the origin of the reciprocal lattice and then constructing a sphere of radius k about the beginning of the vector $\vec{k}$. For any point at which this sphere intersects a reciprocal lattice rod, a line to this point from the center of the sphere represents a diffracted beam $\vec{k}'$. Several such beams are shown in Figure 5.

In RHEED, energies in the range 5-100 keV are used along with grazing incidence. Therefore, the Ewald spheres have very large radii compared to the spacing of the rods in reciprocal space. In addition to this, the rods have a finite thickness. For this reason, RHEED patterns are 'streaked', with each reciprocal net point being represented not by a single diffraction beam but by a diffraction streak. Figure 6 shows a scaled drawing of the RHEED geometry used in our system for 5 KeV electrons incident at 5° to the Si(111) surface along the (110) direction.

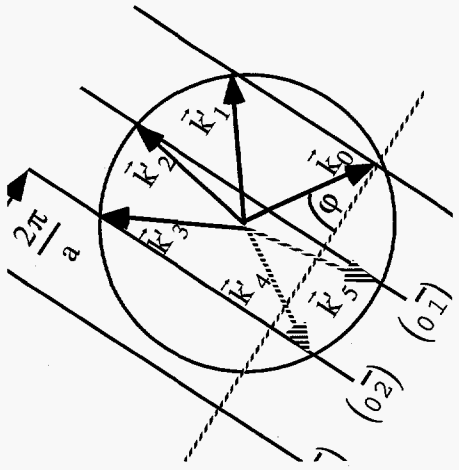

Figure 5. The Ewald sphere construction for a square net of atoms of side a. In the case shown, five elastically scattered diffracted beams can be generated by the incident wave vector $\vec{k}_0$ arriving at an angle of incidence φ to the surface. More beams than are shown will actually occur because only the part of reciprocal space in the plane of the paper can be drawn

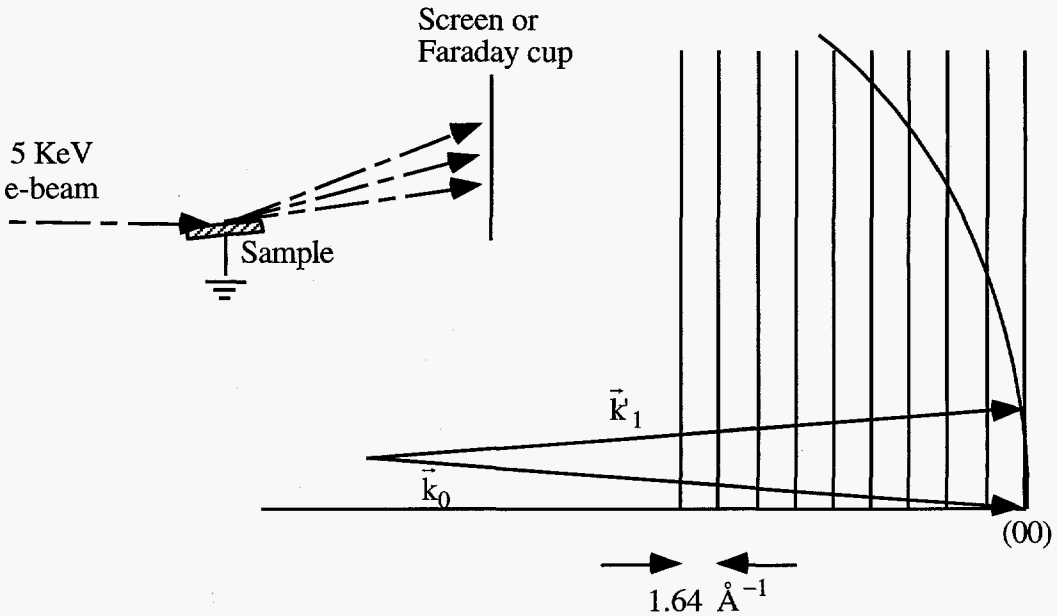

Figure 6. Ewald sphere construction and geometry employed for RHEED. The incident wave vector has magnitude $k_0 = 36.1$ Å^{-1}. For clarity, only the specularly reflected beam has been shown

EXPERIMENTAL APPARATUS

Vacuum Requirements and UHV Chamber

A basic requirement of any study of the properties of a surface at the atomic level is that the surface composition stays essentially constant over the duration of a typical experiment. This means that the experiments should be carried out in an environment where the rate of arrival of reactive species from the surrounding gas phase is low enough to ensure that only a small fraction of an atomic monolayer of atoms sticks to the surface under study. This requirement can be easily evaluated from the kinetic theory of gases[4]: let I be the flux of molecules, that is, the number of molecules per second that crosses a unit area. Assuming a unit surface with normal along the x axis, the contribution to the flux from molecules of velocity $\vec{v}$ is

$$dI = d^3p v_x f(\vec{p}).$$

Assuming the Maxwell-Boltzman distribution for $f(\vec{p})$, we have

$$I = \frac{nm^3}{(2\pi mkT)^{3/2}} \int_0^\infty dv_x v_x e^{-mv_x^2/2kT} \int_{-\infty}^\infty dv_y e^{-mv_y^2/2kT} \int_{-\infty}^\infty dv_z e^{-mv_z^2/2kT}$$

so

$$I = n\sqrt{\frac{kT}{2\pi m}} = \frac{n\bar{v}}{2\sqrt{\pi}}$$

or eliminating n through P=nkT,

$$I = \frac{P}{\sqrt{2\pi mkT}}.$$

Typically, the environment for surface experiments is made up of residual amounts of hydrogen and other gases. For a surface of area A=1 cm^2, 1 ML corresponds to about 10^{15} atoms. If we need to restrict the formation time of a monolayer, τ, to about 1 hour (typical length of an experiment), assuming that all molecules arriving to the surface stick to it, we obtain for the pressure

$$P = \frac{\sqrt{2\pi(2.3\times10^{-26}\,\mathrm{kg})(1.4\times10^{-23}\,\mathrm{JK^{-1}})(300\mathrm{K})}(10^{15}\,\mathrm{at.})}{(3600\mathrm{s})(10^{-4}\,\mathrm{m^2})} = 6.8\times10^{-8}\,\mathrm{Pa} \approx 10^{-10}\,\mathrm{torr}.$$

This pressure belongs in the Ultra High Vacuum (UHV) range. The use of building materials in UHV is restricted to only those with very low vapor pressure such as Stainless Steel, OFHC Copper and Alumina (Aluminum Oxide) as an insulating material. In addition, in order to obtain UHV the whole experimental apparatus must be 'baked'. This initially increases the rate of desorption of the inner walls and instrument surfaces within the chamber and decreases the surface coverage. After cooling the chamber to room temperature, the desorption rate is decreased along with the gas load in the vacuum pumps, making it possible to achieve lower pressures. Our UHV system consists of a Stainless Steel vessel with flanged ports sealed with Cu gaskets. A 60 l/s turbomolecular pump allows us to achieve pressures in the 10^{-10} torr range after baking at 200 °C for 48 hours.

Components and Instrumentation

Sample manipulation

The sample is mounted on an OFHC-Cu sample holder fitted with a W-3%Rh/W-25%Rh thermocouple. The sample holder is attached to a wobble stick manipulator allowing longitudinal, rotational and vertical motions. The sample can be resistively heated by a current limited power supply. The temperature of the surface can be monitored by a thermocouple up to 500°C and by an infrared pyrometer above this temperature within 1°C. Figure 7 shows the sample motions and connections.

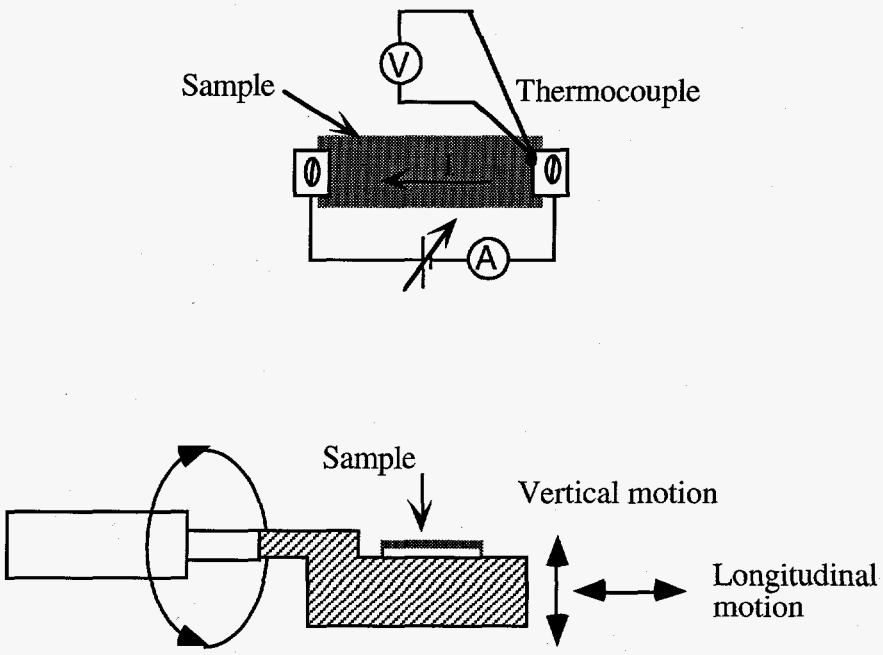

Figure 7. Sample connections and motions

Faraday cup

A Faraday cup was designed and built by us to measure only the elastic portion of the diffracted beams. The collector is a deep and hollow cylinder. The dimensions have been chosen so as to minimize the effect of secondary emission at the collector. The depth of the collector should roughly be at least five times its diameter. The collector is connected to the 'High' input of an electrometer able to measure currents down to 0.01 pA, and can be biased through a high voltage power supply in order to prevent inelastically scattered electrons from being counted. Thus, only the elastically scattered part of a diffracted beam current can be measured. Extreme precautions have to be taken to avoid leakage currents from the biased collector to ground. In practice, leak currents are avoided by guarding the collector with a conductor at the same biasing potential. Figures 8 and 9 demonstrate why guarding is essential to measure the small beam currents. In Figure 8, a non-guarded configuration is shown. Even though the insulators used have high electrical resistance ($R_{ins} \sim 10^{14} \Omega$) a 5 kV biasing in the collector can produce a leak current $I_L \sim 50$ pA, well within the range of diffracted beam currents. The current through the meter, I_M, contains both the beam and leak currents. Figure 9 shows a guarded configuration. In this case, the collector is fully guarded through a cylinder so that only the electrometer burden voltage (~200 μV) appears across R_{ins}, and I_L is virtually reduced to zero.

The electrometer has an analog output that has been used to drive a chart recorder through an isolation amplifier. The Faraday cup has been mounted in a manipulator to allow rotary and linear motion. Positioning of the collector to measure the beam current of a RHEED spot is achieved through these movements and a phosphor screen with a small centered aperture attached to the front of the Faraday cup. Figure 10 is a diagram of the complete assembly.

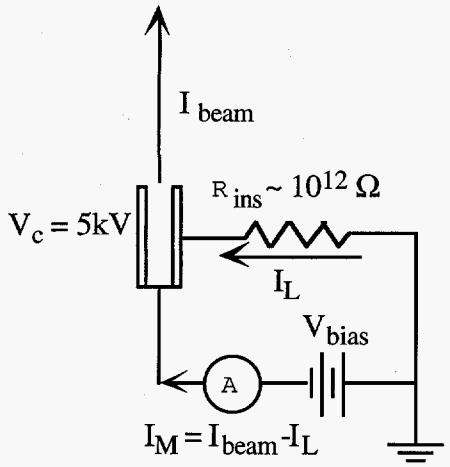

Figure 8. Unguarded configuration

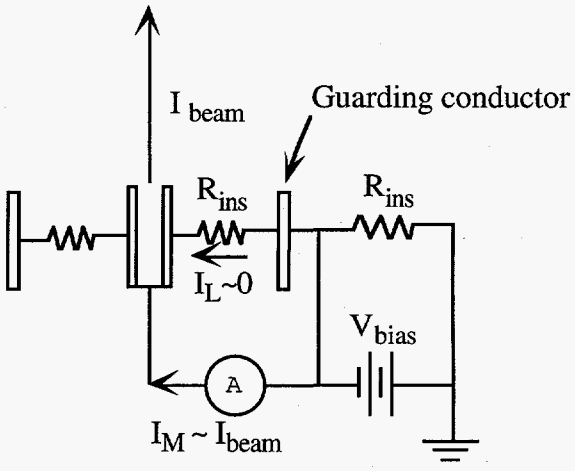

Figure 9. Guarded configuration

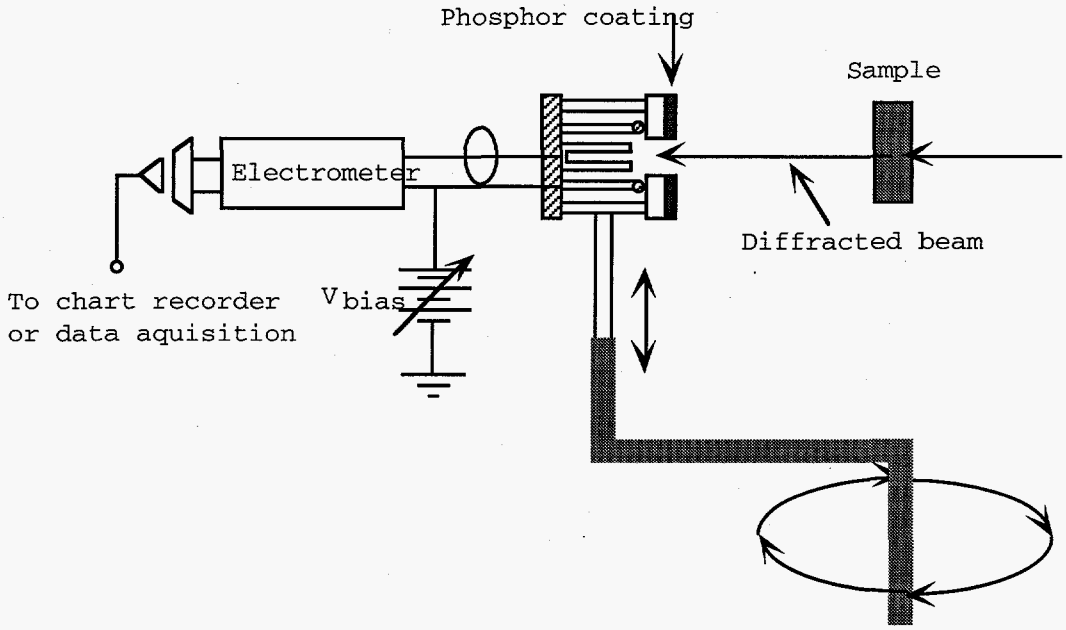

Figure 10. Faraday cup motions and connections

Effusion cell

An effusion cell or Molecular Beam Epitaxy (MBE) source has been mounted to study epitaxial growth of Ag on Si. The cell is electrically heated and it is possible to perform depositions of Ag with fluxes as slow as 1/4800 ML/s. The calibration of the cell is important. There are different means to achieve this. For instance, commercially available quartz monitors can measure the thickness of a film or the flux rate of a source by relating the shift in the resonance frequency of a quartz crystal to the amount of a species deposited on it.

Geometry of the experimental apparatus

The arrangement and distribution of the different components is critical when designing a RHEED apparatus. In addition to the grazing incidence requirement, care must be taken that the diffraction pattern fits on a suitable size screen and that it is visible by the eye. Also, when performing epitaxial growth, the MBE source must face the sample in an unobstructed manner. Figure 11 is a schematic diagram of our arrangement.

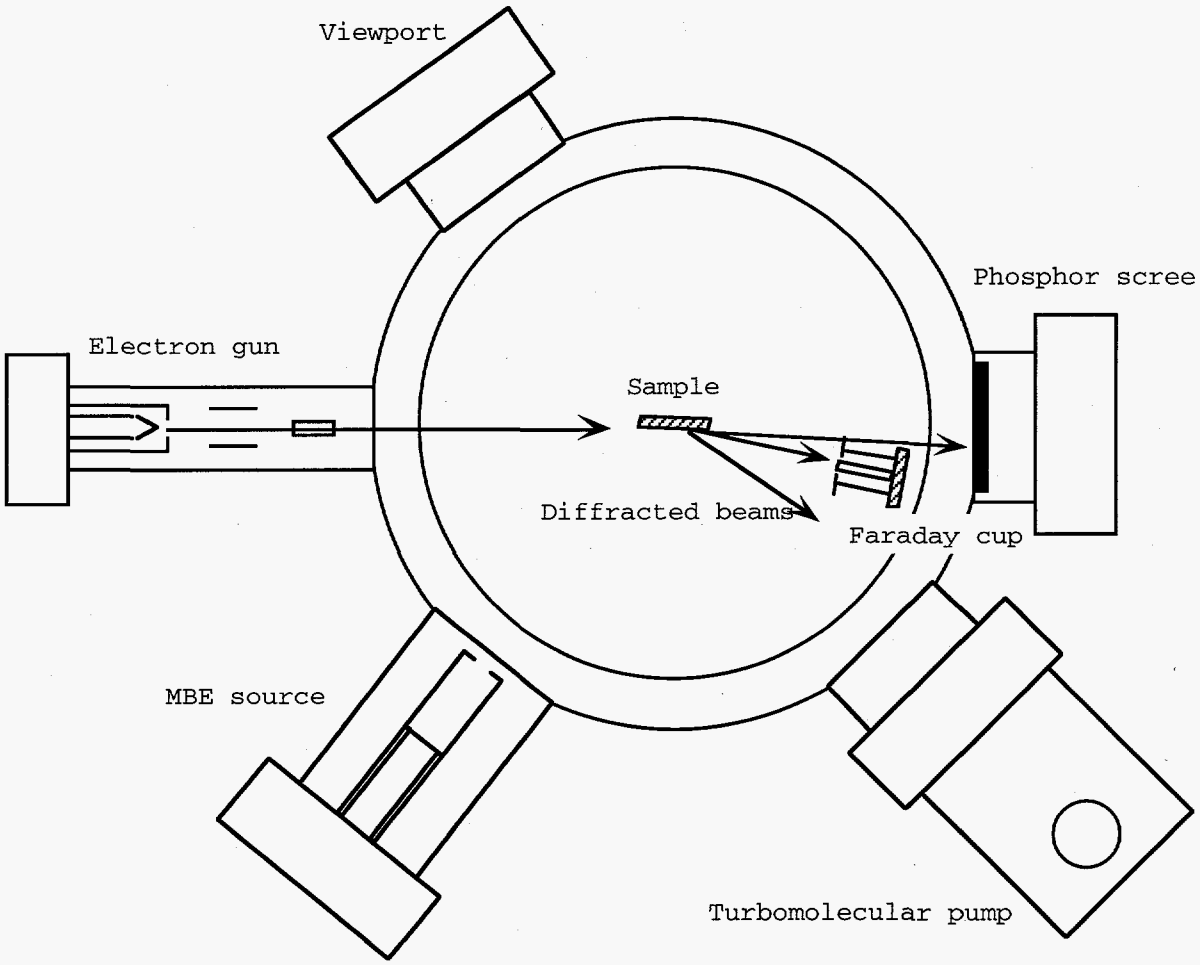

Figure 11. Schematic diagram of our RHEED set-up

EXPERIMENTAL RESULTS

In order to test the performance of our RHEED set-up, we have performed two kinds of measurements: first, we have deposited Ag/Si(111) at different rates and have monitored the diffracted current of the specularly reflected beam with the Faraday collector unbiased, and second, we have tested the capability of the Faraday cup to measure only the elastically scattered part of the diffracted beams.

Ag Deposition

Before actually depositing silver on the silicon surface, it is necessary to guarantee the cleanliness and smoothness of the substrate. As it was previously pointed out, one way to do this is obtaining the Si(111)7x7 structure. This structure was induced by first outgassing the specimen at about 500 °C for a few hours to desorb water and hydrocarbons, then outgassing at 850-900 °C to desorb SiO_2 and finally flashing the sample at 1200°C for two minutes and annealing at 400°C for five more minutes(8). During the degassing process, the vacuum must be at least 1×10^{-9} torr.

After obtaining the Si(111)7x7 structure, depositions at room temperature with different fluxes were made. The specular beam current is shown as a function of the deposition time for four different flux rates in Figure 12. It can be observed that the diffracted current drops to about 50% of its initial value in a characteristic time that depends on the flux used. The minimum value attained by the current corresponds to the diffuse background observed in the diffraction pattern. This value seems somewhat bigger than the one normally observed when using a phosphor screen and a video camera for intensity measurements because the Faraday collector is much more sensitive, especially for low energy electrons, and because the Faraday collector is closer to the sample than a RHEED screen normally is. The absence of oscillations in the current reveals that the growth is not layer by layer. A characteristic time τ for the

growth process can be used to check the temperature behavior of the MBE source. To do this we note that the flux F is inversely proportional to the time τ. The calculation to obtain the flux of particles at a given temperature and pressure has been carried out already when discussing the vacuum requirements for a surface experiment. The result is that the flux at the sample can be written as

$$\frac{F}{a} = \frac{Ae^{CT}}{\pi L^2 \sqrt{2\pi mkT}}$$

where the exponential factor corresponds to the behavior of the vapor pressure of Ag and a and L are geometrical constants. In practice, the constants A and C are such that the exponential almost totally masks the $T^{-1/2}$ factor for the temperatures of interest (600-1000°C). For Ag, C~0.023 $°C^{-1}$ and A~$5x10^{-13}$ torr. Therefore the behavior of the flux should be almost entirely exponential in the temperature as can be seen from Figure 13, which has been obtained using the characteristic time τ obtained from the different runs in Figure 12.

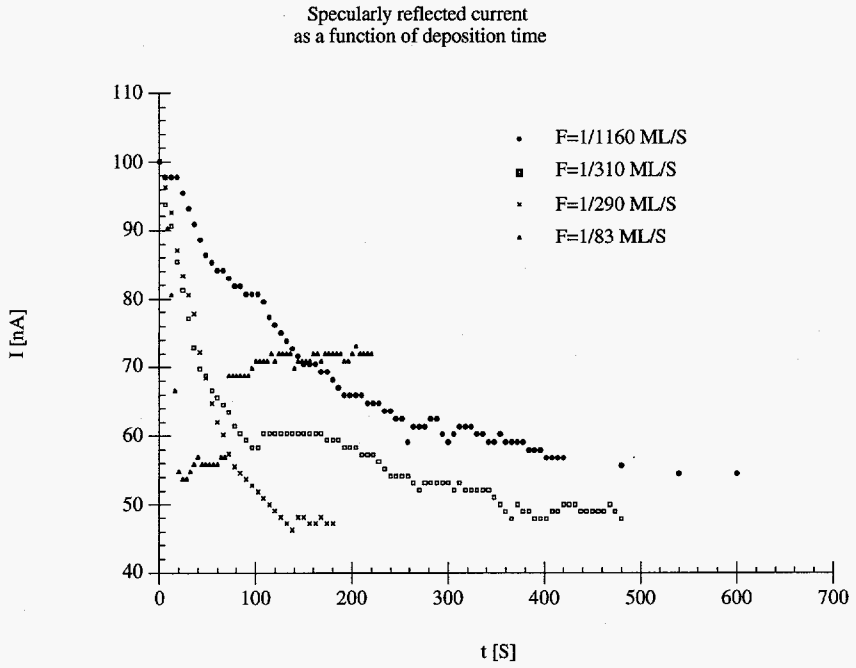

Figure 12. The specularly diffracted current as a function of the deposition time

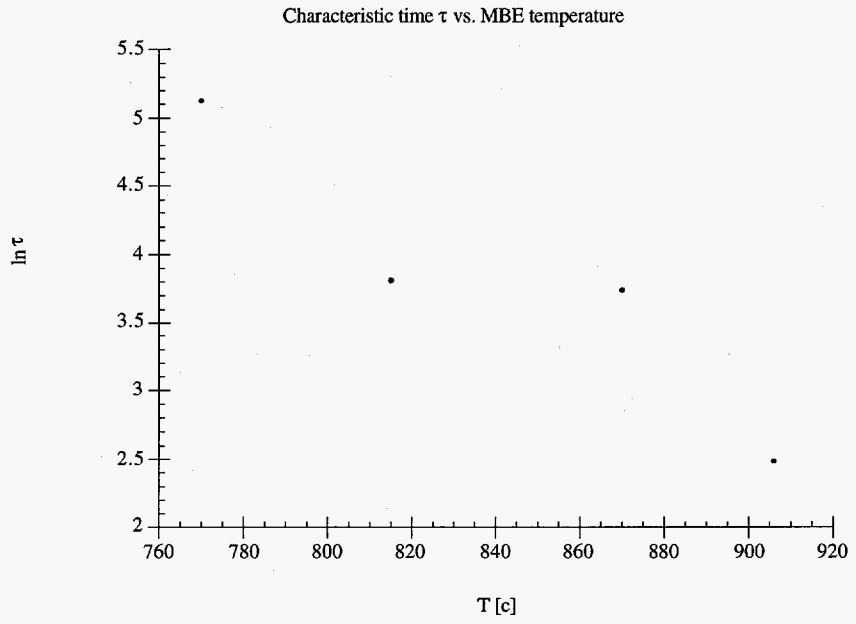

Figure 13. Exponential behavior of the flux

Elastic Scattering Measurements

The main purpose of using a Faraday cup is to provide information exclusively from the elastically scattered part of a diffraction beam. In our last experiments we have tried two different sets of collectors that differ only in the size of their cavities. It was experimentally determined that the collector with the smaller cavity produces unacceptable levels of secondary emission that cannot be trapped inside the collector. This produces partial cancellation of the diffracted current, making extremely inaccurate measurements of the elastic portion. After a deeper collector was installed, measurements of diffracted spots revealed much less secondary emission leaving the collector, and the elastic part of the specular beam was estimated to be about 10% of the total current. Figure 14 is a graph of the specularly reflected beam current as a function of the collector bias. The accelerating voltage in the electron gun was held at 2.6 kV. It can be noticed that initially there is a drop of about 30% in the current with only a few hundreds eV. This is due to the fact that the true secondary and Auger electrons have energies no bigger than 100 eV. The plateau contains the elastic and quasi elastic electrons. These have either been elastically scattered or have lost energy with phonons. Figure 15 is a plot of the derivative of the diffracted current as a function of the collector bias. This derivative is proportional to the energy spectrum of the electrons in a diffracted beam and confirms our previous statements[2].

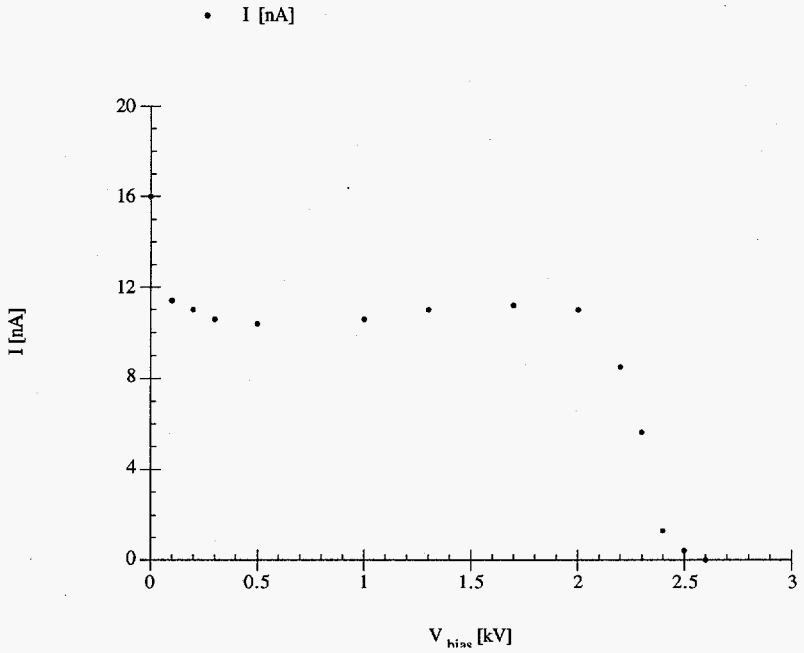

Figure 14. Detected specularly diffracted current as a function of the collector biasing voltage

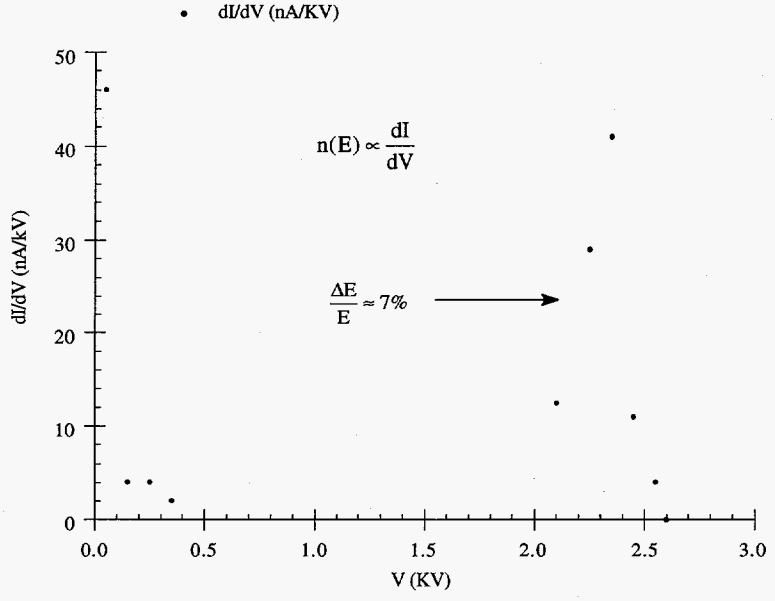

Figure 15. The derivative of the diffracted current

CONCLUSIONS

We have set up an experimental apparatus to study the role of elastic scattering in RHEED from atomically flat surfaces. It has been determined that the Faraday cup can effectively discriminate against inelastic scattering. The collector can measure the current (intensity) of a single spot. Diffracted currents in the range 10^{-10}-10^{-8} Amp have been measured, and it is expected that capabilities of the collector extend to 10^{-12} Amp. The experimental apparatus can also be used to carry in-situ studies of thin film growth by MBE (Molecular Beam Epitaxy).

BIBLIOGRAPHY

1. Aschcroft, N. W.; Mermin, N. D. Solid State Physics; W. B. Saunders Company: New York, 1976.

2. Baroody, E. Physical Review 1950, 78(6), 780-787.

3. Gotoh, Y.; Ino, S. Japanese Journal of Applied Physics 1978, 17(12), 2097-2109.

4. Huang, K. Statistical Mechanics, 2nd ed.; John Wiley & Sons: New York, 1987.

5. Kittel, C. Introduction to Solid State Physics, 6th ed.; John Wiley & Sons Inc.: New York, 1986.

6. Marten, H. Proceedings of the NATO Advanced Research Workshop in Reflection High Energy Electron Diffraction and Reflection Electron Imaging of Surfaces, Veldhoven, the Netherlands; Plenum Press: New York, 1987; 109-115.

7. Prutton, M. Surface Physics; Clarendon Press: Oxford, 1975.

8. Swartzentruber, B. S.; Mo, Y.-W.; Webb, M.B.; Lagally, M.G. Journal of Vacuum Science Technology A 1989, 7(4), 2901-2907.

9. Zangwill, A. Physics at surfaces; Cambridge University Press: New York, 1988.

ACKNOWLEDGMENT

This work was performed at Ames Laboratory under Contract No. W-7405-eng-82 with the U.S. Department of Energy. The United States government has assigned the DOE Report number IS-T 1734 to this thesis.